The EMBO Journal Vol.18 No.9 pp.2352–2363, 1999

The specificity of polygalacturonase-inhibiting protein (PGIP): a single amino acid substitution in the solvent-exposed β-strand/β-turn region of the leucine-rich repeats (LRRs) confers a new recognition capability

F.Leckie, B.Mattei, C.Capodicasa, A.Hemmings[1], L.Nuss, B.Aracri, G.De Lorenzo and F.Cervone[2]

Dipartimento di Biologia Vegetale, Università di Roma 'La Sapienza', Piazzale Aldo Moro 5, 00185, Roma, Italy and [1]Schools of Biological and Chemical Sciences, University of East Anglia, Norwich NR4 7TJ, UK

[2]Corresponding author
e-mail: cervone@axrma.uniroma1.it

Two members of the *pgip* gene family (*pgip-1* and *pgip-2*) of *Phaseolus vulgaris* L. were expressed separately in *Nicotiana benthamiana* and the ligand specificity of their products was analysed by surface plasmon resonance (SPR). Polygalacturonase-inhibiting protein-1 (PGIP-1) was unable to interact with PG from *Fusarium moniliforme* and interacted with PG from *Aspergillus niger*; PGIP-2 interacted with both PGs. Only eight amino acid variations distinguish the two proteins: five of them are confined within the β-sheet/β-turn structure and two of them are contiguous to this region. By site-directed mutagenesis, each of the variant amino acids of PGIP-2 was replaced with the corresponding amino acid of PGIP-1, in a loss-of-function approach. The mutated PGIP-2s were expressed individually in *N.benthamiana*, purified and subjected to SPR analysis. Each single mutation caused a decrease in affinity for PG from *F.moniliforme*; residue Q253 made a major contribution, and its replacement with a lysine led to a dramatic reduction in the binding energy of the complex. Conversely, in a gain-of-function approach, amino acid K253 of PGIP-1 was mutated into the corresponding amino acid of PGIP-2, a glutamine. With this single mutation, PGIP-1 acquired the ability to interact with *F.moniliforme* PG.

Keywords: leucine-rich repeat proteins/molecular recognition/polygalacturonase-inhibiting protein (PGIP)

Introduction

Polygalacturonase-inhibiting proteins (PGIPs), present in the cell walls of many plants (Cervone *et al.*, 1997), belong to the large family of leucine-rich repeat (LRR) proteins. At present, >100 LRR proteins of diverse origin (microbia, animals and plants) have been described. The LRR is a versatile structural motif responsible for many protein–protein interactions and involved in many different cell functions such as receptor dimerization, domain repulsion, regulation of adhesion and binding events (Buchanan and Gay, 1996).

In the few cases investigated so far, the importance of LRRs for interaction with other molecules has been clearly assessed. For example, the specific binding sites of decorin, a protein belonging to the proteoglycan family, for collagen type I have been localized within the sixth LRR, where a single mutation, E180K, is responsible for a major diminution in binding (Kresse *et al.*, 1997). Hormone binding of the lutropin–choriogonadotropin receptor (LH/CG-R) (G-protein-coupled receptors) was localized within the LRRs 1–6 of the receptor (Puett *et al.*, 1996; Thomas *et al.*, 1996).

A significant advance in understanding the structural basis of LRR-mediated molecular interactions comes from crystallographic studies of the ribonuclease inhibitors (RI). Co-crystallization of porcine RI (pRI) and human placental RI (hRI) with RNase A and angiogenin (Ang), respectively, has been achieved (Kobe and Deisenhofer, 1996; Papageorgiou *et al.*, 1997). In these proteins, a repeated β-strand/β-turn structure is determined by the presence in each LRR module of the motif xxLxLxx, where the leucine residues form a hydrophobic core, while the side chains of the amino acids flanking the leucines are solvent exposed and interact with the ligands (Kobe and Deisenhofer, 1993, 1995). Twenty six out of 28 contact points between pRI and RNase A occur in the β-strand or β-turn region of the LRRs; similarly, 25 of the 26 contact points between hRI and Ang are located in the β-strand or β-turn region. The majority of the hydrogen bonds and van der Waals contacts in the two complexes are distinctive, indicating that the ability of the inhibitor to recognize different ligands is based on its ability to interact with a number of features unique to each of them (Papageorgiou *et al.*, 1997). However, a thorough analysis of the contribution of the single amino acids in the RI–RNase interactions is difficult, due the high number of contacts established in the complexes.

In plants, LRR proteins play a relevant role in both development and defence, where specificity of recognition is a fundamental prerequisite. These proteins include PGIPs, the products of the resistance (*R*) genes *Cf* of tomato, which confer resistance to different races of the fungus *Cladosporium fulvum* (Hammond-Kosack and Jones, 1997), and *Xa21* of rice, which confers resistance to *Xanthomonas oryzae* pv. *oryzae* (Wang *et al.*, 1996), as well as several orphan receptor kinases involved in *Arabidopsis* development, such as ERECTA (Torii *et al.*, 1996), CLAVATA1 (Clark *et al.*, 1997) and a putative receptor for brassinosteroids (Li and Chory, 1997). All these proteins share LRRs of the extracellular or extracytoplasmic type, characterized by the consensus sequence LxxLxxLxLxxNxLT/SGxIPxxLGx (Kajava, 1998), and a similarity not only in the LRR region but also in the regions outside the LRR domain (Bent, 1996; De Lorenzo and Cervone, 1997). Although to a lesser extent, PGIPs also share similarity with *R* gene products characterized

by LRRs of the intracellular type (Hammond-Kosack and Jones, 1997).

Because *R* gene products are thought to function as receptors for pathogen-encoded avirulence (Avr) proteins, it has been hypothesized that sequence variation within LRRs influences recognition specificity. Comparison of members of the *Cf* family has identified the β-sheet/β-turn region as a 'hypervariable' region, probably responsible for the ligand specificity in this class of proteins (Parniske *et al.*, 1997). However, analysis of the molecular basis of recognition specificity either in the *R* gene products or in the development-related LRR receptors is not yet possible because the nature of the ligands for the latter is still unknown, while the evidence for a direct molecular interaction between an LRR R protein and an *avr* product is still awaited. Given their close structural relationship to these proteins, PGIPs and their ligands, polygalacturonases (PGs), represent a unique model system for studying the structural bases of recognition specificity of plant LRR proteins. This knowledge can be exploited for designed manipulation of the LRR structure to generate new specific molecular interactions for the control of developmental processes or the creation of new resistance traits in plants.

PGIPs interact with fungal endopolygalacturonases and inhibit their enzymatic activity *in vitro* (De Lorenzo and Cervone, 1997). The proteins isolated from bean (Cervone *et al.*, 1987), pear (Stotz *et al.*, 1993), raspberry (Johnston *et al.*, 1993), tomato (Stotz *et al.*, 1994) and soybean (Favaron *et al.*, 1994) have differential inhibition spectra towards a range of PGs from phytopathogenic fungi. Different inhibitory activities against PGs have also been observed in PGIPs from a single plant source (Desiderio *et al.*, 1997), indicating that *pgip* genes have undergone diversification during evolution.

Like many plant *R* genes, *pgip* genes are organized into complex multigene families. In *Phaseolus vulgaris*, the *pgip* gene family consists of at least five members and perhaps as many as 15 (Frediani *et al.*, 1993). Previous data suggest that different members of the family encode PGIPs with nearly identical biochemical characteristics but distinct specificity, i.e. the ability to interact with different fungal PGs (Desiderio *et al.*, 1997). We have now searched for and isolated, from a cDNA library of *P.vulgaris* cv. Pinto, two members of the *pgip* gene family (*pgip-1* and *pgip-2*), which, within the coding regions, differ by only 26 nucleotides. Upon expression in *Nicotiana benthamiana*, we have investigated by surface plasmon resonance (SPR) the ligand specificity of the encoded proteins before and after site-directed mutagenesis to evaluate the energetic parameters of individual interface contributions, which cannot be gained from crystallographic data. Here, we report the distinct ability of PGIP-1 and PGIP-2 to recognize fungal PGs, and on the role and contribution of the single amino acids that distinguish PGIP-1 and PGIP-2 in the specific interactions with PGs from *Aspergillus niger* and *Fusarium moniliforme*. Our results show that the residues determining the recognition specificity of PGIP reside in the region flanking the predicted β-sheet/β-turn structure of the protein, and that a single amino acid variation in the β-strand/β-turn motif can confer to PGIP a new recognition capability.

Results

Isolation and characteristics of the pgip clones

A cDNA library from suspension-cultured cells of *P.vulgaris* cv. Pinto was screened using as a probe the genomic *pgip* clone previously isolated from a library of *P.vulgaris* cv. Saxa (Toubart *et al.*, 1992). Seventeen clones were purified and subjected to restriction enzyme digestion and Southern blot analysis; the 10 longest inserts were subcloned in the *Sal*I–*Eco*RI site of the pBlueScript SK+ plasmid and sequenced. Since previous data had shown that PGIPs with different specificities have indistinguishable biochemical characteristics, suggesting that different *pgip* genes might be highly similar (Desiderio *et al.*, 1997), even a few nucleotide differences among the cDNAs were not neglected and were confirmed carefully. All the 10 sequenced cDNAs exhibited a poly(A) tail and could be grouped into two classes, each corresponding to a distinct *pgip* gene. Within each class, cDNAs had completely matching nucleotide sequences but different lengths, because, being partial cDNAs, they differed at their 5′ ends. One class included four cDNAs and corresponded to a gene, *pgip-1*, identical and co-linear with the genomic *pgip* clone from *P.vulgaris* cv. Saxa (Toubart *et al.*, 1992); within this class, only one clone contained the two in-frame ATGs described in the Saxa *pgip* clone, while the other three cDNAs were shorter. The other class (six cDNAs) corresponded to a different gene, named *pgip-2*, that shares a high degree of identity with *pgip-1* (99.1% in the coding region). The longest cDNA started with an ATG, corresponding to the second ATG of *pgip-1* (Figure 1).

Nucleotide changes (a total of 26, resulting in 10 amino acid changes between PGIP-1 and PGIP-2) are more frequent in the region encoding the C-terminal half of the LRR domain (Table I). A high number and a particular distribution of non-synonymous (11/26) substitutions compared with synonymous (15/26) substitutions can be observed. Furthermore, as shown in Figure 1, seven of the 11 non-synonymous substitutions lead to amino acid differences which are located in the LRR domain: five of these are internal to the xxLxLxx motif predicted to form the solvent-exposed β-sheet/β-turn structure of the protein, while two other amino acid substitutions are very close to this region and their side chains presumably are also solvent exposed. Each LRR contains only one variation, and some LRRs (the second, third, fourth, seventh and ninth) are invariant between the two proteins. The remaining three variant amino acids are outside the LRR domain: two are located in the signal peptide of the protein and therefore do not affect the structure of the mature protein, and one resides in the C-terminal region of the protein. Instead, most synonymous nucleotide changes correspond to residues located outside the β-sheet/β-turn structural motif.

In order to evaluate the possible functional significance of the point mutations and the subsequent amino acid changes, the relative mutability of the variant amino acids between PGIP-1 and PGIP-2 was analysed according to Dayhoff *et al*. (1972) by comparing their rate of acceptance within protein families which display point mutations. The more acceptable an interchange is between two amino acids, the more frequent it is, and this depends on the

chemical and physical similarities between the amino acids. Conversely, a low rate of acceptance should be a rare event and is indicative of a selection pressure in favour of diversification. Substitutions with a low rate of acceptance are typical of proteins involved in recognition functions. Some of the variations between PGIP-1 and PGIP-2 have a low rate of acceptance: in particular, the variations G181V and K253Q, occurring within the putative β-sheet/β-turn motif, and H89L and K320Q, contiguous to this structural motif, are low or moderately accepted. Instead, variations S326A and S340A, as well as variations Q300H and A207S, both have a high rate of acceptance, and are not expected to determine major functional differences.

Inhibition specificity of PGIP-1 and PGIP-2

The inhibitory activity of bulk bean PGIP is a composite of the activities of several PGIPs (Desiderio *et al.*, 1997). In order to analyse the individual contribution of PGIP-1 and PGIP-2 to the total inhibition spectrum, the complete coding sequences of the genes *pgip-1* and *pgip-2* were introduced separately into the expression cassette of the virus vector based on potato virus X (PVX) (Baulcombe *et al.*, 1995) to create PVX.PGIP-1 and PVX.PGIP-2 for transient expression in *N.benthamiana* as previously described (Desiderio *et al.*, 1997). The putative leader or signal peptide sequence from nucleotide +1 to +27 of *pgip-1* was also added to *pgip-2* as this sequence may be important for high level expression of the protein (Devoto *et al.*, 1998). Western blot analysis of crude protein extracts from symptomatic plants inoculated with PVX.PGIP-1 and PVX.PGIP-2 demonstrated the presence of a PGIP-specific signal with a molecular mass of 39 kDa which was absent in wild-type extracts (data not shown).

After purification to homogeneity from *N.benthamiana* extracts, the ability of increasing amounts of PGIP-1 and PGIP-2 to inhibit PGs from different fungi was investigated. PGIP-1 showed a specificity spectrum very similar to that reported for PGIP-1 from cv. Saxa (Desiderio *et al.*, 1997): 30 ng inhibited the homogeneous PG from *A.niger* at almost 100%, but did not inhibit a homogeneous PG of *F.moniliforme* expressed in *Saccharomyces cerevisae* (Caprari *et al.*, 1996), and had a reduced ability to inhibit crude preparations of PG from *Fusarium oxysporum* f.sp. *lycopersici* and *Botrytis cinerea*. PGIP-2 (30 ng) almost completely inhibited all PGs used, with the exception of PG from *F.oxysporum* f.sp. *lycopersici* which was only partially inhibited (60%) (Figure 2). Therefore, PGIP-2 exhibits a broader spectrum of interactions than PGIP-1, and shows an interaction feature absent in PGIP-1, i.e. the ability to recognize *F.moniliforme* PG.

The interaction between purified PGIP-1 and PGIP-2,

Fig. 1. Top: nucleotide sequence alignments of the coding sequences of *pgip-1* and *pgip-2* isolated from a *P.vulgaris* cv. Pinto cDNA library. For *pgip-2*, only nucleotides that differ from *pgip-1* are indicated. Dots indicate identity. Start and stop codons are indicated in bold. *Hin*dIII and *Mlu*I endonuclease restriction sites are underlined and indicated by H and M, respectively. Bottom: PGIP-2 LRR structure. (**A**), signal peptide; (**B**), presumed N-terminus of the mature protein; (**C**), 10.5 LRRs; and (**D**), C-terminus. Putative glycosylation sites are indicated by an asterisk. The box indicates the area of the protein predicted to form the β-sheet/β-turn structural motifs. Based on the comparison between *pgip-1* and *pgip-2*, amino acid residues corresponding to synonymous nucleotide changes are indicated in bold, those corresponding to non-synonymous variations are highlighted. Amino acids are numbered according to the corresponding residues of PGIP-1 (see also the footnotes to Table I).

Table I. Amino acids which distinguish PGIP-1 from PGIP-2[a]

Amino acid position	PGIP-1	PGIP-2
26	R	S
29	L	H
89	H	L
181	G	V
207	A	S
253	K	Q
300	Q	H
320	K	Q
326	S	A
340	S	A

[a]The amino acid position refers to the residue in PGIP-1. Since the cDNA clone coding for PGIP-2 contains only one methionine codon corresponding to amino acid position 10 in PGIP-1, the amino acid position 26 in PGIP-1 corresponds to the amino acid position 17 in PGIP-2.

and homogeneous *A.niger* and *F.moniliforme* PGs, was examined by using a biosensor based on SPR (Granzow and Reed, 1992; Schuster *et al.*, 1993). PGIP-1 and PGIP-2 were immobilized as ligands on sensor surfaces while PGs were passed in solution as analytes over the surface. The interactions between PGIP-1 or PGIP-2 with increasing amounts of the two PGs were analysed kinetically. PGIP-1 was unable to interact with *F.moniliforme* PG, and showed an affinity towards *A.niger* PG (K_D = 62.1 nM) comparable with that of PGIP-1 from cv. Saxa (K_D = 40 nM) (Desiderio *et al.*, 1997). Instead, PGIP-2 interacted with both enzymes. In comparison with PGIP-1, PGIP-2 showed a much higher affinity for *A.niger* PG (K_D = 0.96 nM) and had the capacity to interact with *F.moniliforme* PG (K_D= 47.7 nM) (Figure 3; Tables II and III).

Analysis of domain-swapped PGIPs

In order to understand which region of PGIP-2 is responsible for recognition of *F.moniliforme* PG, we swapped domains between PGIP-1 and PGIP-2, exploiting the presence of a restriction enzyme site, *Mlu*I, in the coding region of both genes (Figure 1). The region of *pgip-2* encoding the N-terminal portion (nucleotides 1–722, corresponding to amino acids 1–241) was replaced with the corresponding portion of *pgip-1* to create *pgip-12*, and vice versa to create *pgip-21*. The sequences encoding the swapped PGIPs were introduced separately into the PVX vector. Following expression in *N.benthamiana*, the chimeric proteins were purified and analysed by SPR using *A.niger* and *F.moniliforme* PGs as analytes. SPR analysis showed that PGIP-21 does not interact with *F.moniliforme* PG (Figure 3; Tables II and III) and, in comparison with PGIP-2, exhibits an affinity 10-fold lower for the *A.niger* PG. Instead, PGIP-12 interacts with both enzymes, and exhibits, in comparison with PGIP-2, affinities 4- and 13-fold lower towards *F.moniliforme* and *A.niger* PGs, respectively. Increased K_D values are due to changes in both k_{on} and k_{off} for PGIP-12, and in k_{off} alone for PGIP-21. We concluded that although residues crucial for the interaction with the *F.moniliforme* PG are located in the C-terminal half of the LRR domain, residues in the N-terminal region also contribute, albeit weakly, to the interaction.

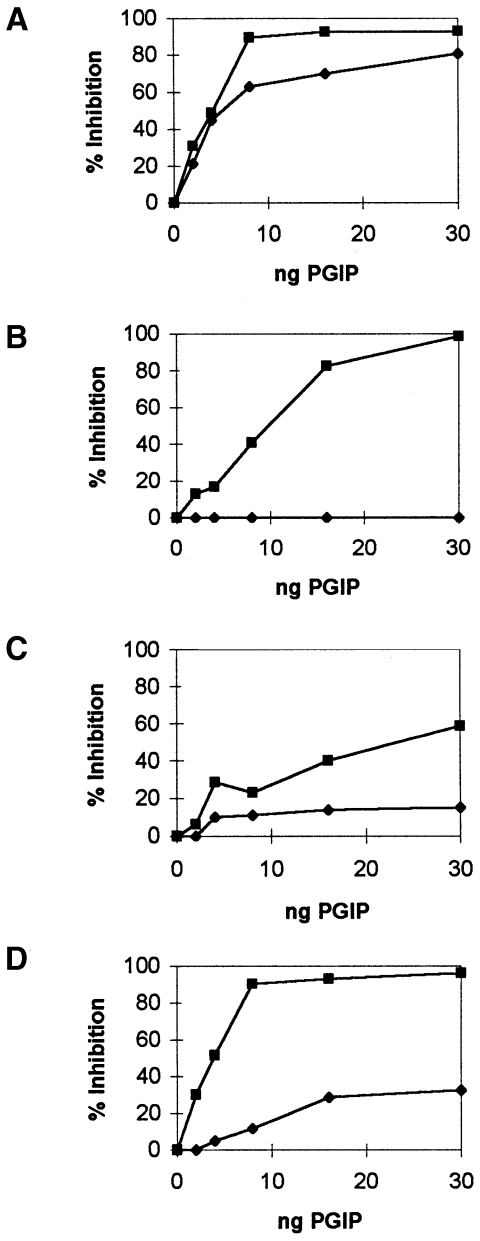

Fig. 2. Inhibition of various fungal PGs by increasing amounts of PGIP-1 (◆) and PGIP-2 (■). The enzymes used were: 0.015 U of homogeneous *A.niger* PG (**A**), 0.008 U of homogeneous *F.moniliforme* PG (**B**), 0.01 U of a crude PG preparation from *F.oxysporum* f.sp. *lycopersici* (**C**) and 0.004 U of a crude PG preparation from *B.cinerea* (**D**).

Site-directed mutagenesis of PGIP-2: analysis with PG of F.moniliforme

The contribution of each single amino acid to the interaction with *F.moniliforme* PG was studied by mutating, in a loss-of-function approach, each of the variant amino acids of PGIP-2 into the corresponding residue of PGIP-1. Thus a series of eight mutated *pgip*-2 genes were created and expressed in *N.benthamiana*. The encoded proteins were purified and individually immobilized on separate sensor chips for analysis by SPR with *F.moniliforme* PG as analyte. The SPR data (Figure 4; Table II) showed that mutation Q253K strongly affects the interaction. The kinetic constants could not be calculated due to the very weak interaction between the mutated protein and the

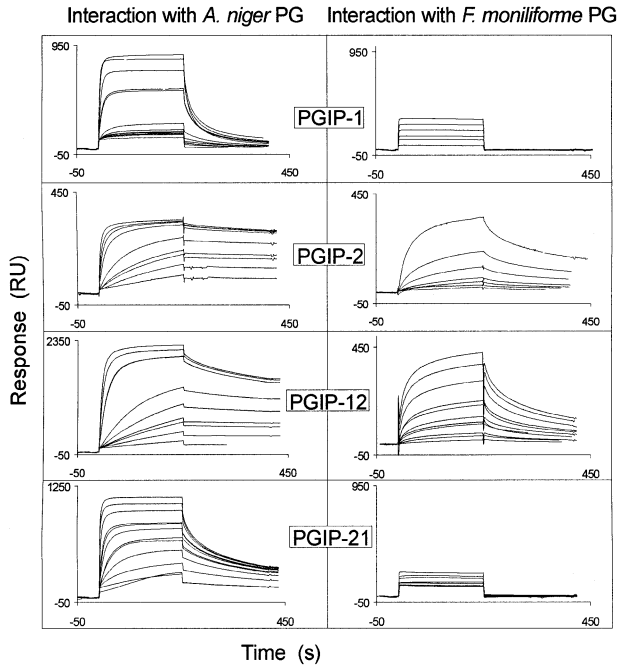

Fig. 3. Interactions between PGIP-1, PGIP-2 or domain swaps PGIP-12 and PGIP-21, and *A.niger* or *F.moniliforme* PG. The different PGIPs were immobilized separately as ligands on sensor surfaces, and the increasing concentration of PGs indicated below were passed in solution as analytes over the surface. The different panels show the SPR sensorgrams. (Concentrations listed from bottom to top curve.) PGIP-1, concentrations of *A.niger* PG: 6.5, 13, 23, 27, 46, 91, 274, 548 and 822 nM, and 1.1 μM; concentrations of *F.moniliforme* PG: 160, 400 and 800 nM, and 1.6, 3.2 and 4.8 μM. PGIP-2, concentrations of *A.niger* PG: 2.3, 4.6, 11, 23, 46, 114, 228 and 456 nM, and 1.1, 2.3 and 4.6 μM; concentrations of *F.moniliforme* PG: 40, 80, 160, 400 and 800 nM, and 1.6, 3.2, 4.8 and 6.4 μM. PGIP-12, concentrations of *A.niger* PG: 6.5, 13, 23, 26, 46, 91, 274 and 548 nM, and 1.1 μM; concentrations of *F.moniliforme* PG: 40, 80, 160, 240, 320, 440, 640 and 882 nM, and 1.7, 2.6 and 3.5 μM. PGIP-21, concentrations of *A.niger* PG: 6.8, 16, 34, 68, 137, 228 and 685 nM, and 1.1 and 2.3 μM; concentrations of *F.moniliforme* PG: 24, 48, 80, 240, 480 and 800 nM, and 1.2 and 1.6 μM. RU, resonance units.

enzyme: the K_D is at least 70-fold higher than that calculated for the wild-type PGIP-2, with both a decrease in the k_{on} value and an increase in the k_{off} value of the dissociation of the complex. PGIP-2 carrying the mutation A326S also showed a decreased affinity: the K_D is 3.5-fold higher with respect to PGIP-2, mainly due to a decrease in the k_{on}. These data are consistent with the data obtained with the domain-swapped PGIPs, and in particular with the observation that PGIP-21, which contains both mutations Q253K and A326S, does not interact with *F.moniliforme* PG. Other mutations had minor effects: mutation V181G produced a 2-fold decrease in the affinity, and mutations L89H and Q320K caused very little variation in the affinity for the enzyme. Mutations H300Q and A340S had little or no effect on the interaction between PGIP-2 and *F.moniliforme* PG (Figure 4; Table II).

Differences in binding free energies between the *F.moniliforme* PG–wild-type PGIP-2 complex and those of each single mutated protein interacting with *F.moniliforme* PG were calculated from the equation

$$\Delta\Delta G = \Delta G_{mut} - \Delta G_{wt} = - RT\ln (K_{Dwt}/K_{Dmut}).$$

The results are summarized in Table II. The replacement of Q253 with K decreases the binding energy by 2.55 kcal/mol, accounting for much of the binding energy of the complex. The residues A326 and V181 make lesser contributions, and all the other residues do not appear to play important roles.

The importance of the amino acids distinguishing PGIP-2 from PGIP-1 was also studied in inhibition assays using PGIP-2s mutated in one or two amino acids. Sixty nanograms of all PGIP-2 single mutants were able to inhibit *F.moniliforme* PG, with the exception of mutant Q253K, which had a much reduced inhibition activity (30%). The double mutant V181G/Q253K as well as the double mutant Q253K/A326S did not inhibit the enzyme; instead, the double mutant V181G/A326S was able to inhibit *F.moniliforme* PG (Table IV).

Site-directed mutagenesis of PGIP-2: analysis with PG of A.niger

The interactions of the mutated PGIP-2s with *A.niger* PG were also analysed. The mutation V181G caused a 6-fold diminution in affinity due to a pronounced increase in the k_{off} value and a slight decrease in the k_{on} value. Similarly, the mutation Q253K caused a 5-fold diminution in the affinity towards the enzyme mainly affecting the k_{off} value. Mutations Q320K and A340S only caused a slight loss of affinity due to a slight decrease in the k_{on} value, while mutations L89H, S207A, H300Q and A326S did not affect the interaction significantly (Figure 4; Table III).

Differences in binding free energies were also calculated for the interaction with *A.niger* PG (Table III). The mutation Q253K caused a decrease in the binding energy of 1.01 kcal/mol; mutation V181G had a similar effect, while all the other mutations had no significant effect.

Site-directed mutagenesis of PGIP-1

In order to confirm the importance of a glutamine at position 253 in the recognition and inhibition of PG from *F.moniliforme*, the corresponding amino acid of PGIP-1, a lysine, was mutated into a glutamine, in a gain-of-function approach. The K253Q PGIP-1 mutant was expressed in *N.benthamiana* and purified. Inhibitory assays and SPR analysis showed that this single mutation confers to PGIP-1 the ability to inhibit completely the *F.moniliforme* PG (Figure 5) and to form a complex with a binding affinity of 205.7 nM (Figure 6; Table V).

Modelling of PGIP-1 and PGIP-2

Like RI, PGIP is likely to have a parallel stacking of β-strand/β-turns forming a solvent-exposed surface. Construction of the model of *P.vulgaris* PGIP-1 was carried out, using a model of the plant-specific LRR motif derived by Kajava (1998) as a template for the single 24 amino acid LRR. A framework for the structure of PGIP-1 was constructed by replicating this motif structure to give a tandem array of 10 identical LRRs. The sequences of the PGIP-1 LRRs were then aligned manually with the plant-specific LRR consensus sequence. Construction of the starting model for PGIP-2 followed, by simple substitution of the amino acids at positions differing between the two proteins within the LRR domain. Both models were then subjected to energy minimization.

The alignment used to model the PGIP-1 structure is shown in Table VI. The alignment, particularly in the

Table II. Kinetics and equilibrium of the interaction[a] between *F.moniliforme* PG and different PGIPs

	k_{on} (per Ms)	k_{off} (per s)	K_D (nM)	ΔG (kcal/mol)	$\Delta\Delta G = \Delta G_{mut} - \Delta G_w$ (kcal/mol)
PGIP-2 (wt)	4.86×10^4	2.32×10^{-3}	47.7	–9.98	0.00
PGIP-1	_[b]	_[b]	_[b]		
PGIP-12	1.76×10^4	3.78×10^{-3}	215	–9.09	0.89
PGIP-21	_[b]	_[b]	_[b]		
PGIP-2 L89H	3.0×10^4	2.48×10^{-3}	82.6	–9.66	0.33
PGIP-2 V181G	4.44×10^4	4.26×10^{-3}	96	–9.57	0.41
PGIP-2 S207A	3.43×10^4	2.9×10^{-3}	84.5	–9.64	0.34
PGIP-2 Q253K	8.2×10^3	2.9×10^{-2}	3536.6	–7.43	2.55
PGIP-2 H300Q	4.22×10^4	2.78×10^{-3}	65.8	–9.79	0.19
PGIP-2 Q320K	1.71×10^4	1.58×10^{-3}	92.4	–9.59	0.39
PGIP-2 A326S	1.57×10^4	2.61×10^{-3}	166.2	–9.24	0.74
PGIP-2 A340S	3.43×10^4	2.23×10^{-3}	65	–9.80	0.18

[a]Kinetic parameters were determined by SPR analysis. K_D values were calculated as k_{off}/k_{on}. The free energy of the formation of the complex was calculated from the equation $\Delta G = RT\ln K_D$. $\Delta\Delta G$ values were calculated from the equation $\Delta\Delta G = -RT\ln(K_{Dwt}/K_{Dmut})$.
[b]No interaction.

Table III. Kinetics and equilibrium of the interaction[a] between different PGIPs and *A.niger* PG

	k_{on} (per Ms)	k_{off} (per s)	K_D (nM)	ΔG (kcal/mol)	$\Delta\Delta G = \Delta G_{mut} - \Delta G_w$ (kcal/mol)
PGIP-2 (wt)	3.89×10^5	3.74×10^{-4}	0.96	–12.30	0.00
PGIP-1	1.01×10^5	6.27×10^{-3}	62.1	–9.83	
PGIP-12	1.07×10^5	1.4×10^{-3}	13.1	–10.75	1.55
PGIP-21	4.41×10^5	4.6×10^{-3}	10.4	–10.89	1.41
PGIP-2 L89H	3.69×10^5	2.9×10^{-4}	0.78	–12.42	–0.12
PGIP-2 V181G	2.38×10^5	1.36×10^{-3}	5.73	–11.24	1.06
PGIP-2 S207A	5.13×10^5	3.2×10^{-4}	0.62	–12.56	–0.26
PGIP-2 Q253K	5.25×10^5	2.79×10^{-3}	5.31	–11.28	1.01
PGIP-2 H300Q	3.6×10^5	2.34×10^{-4}	0.65	–12.53	–0.23
PGIP-2 Q320K	2.35×10^5	3.75×10^{-4}	1.59	–12.00	0.30
PGIP-2 A326S	4.24×10^5	3.74×10^{-4}	0.88	–12.35	–0.05
PGIP-2 A340S	2.43×10^5	3.58×10^{-4}	1.47	–12.04	0.25

[a]Kinetic parameters were determined by SPR analysis. K_D values were calculated as k_{off}/k_{on}. The free energy of the formation of the complex was calculated from the equation $\Delta G = RT\ln K_D$. $\Delta\Delta G$ values were calculated from the equation $\Delta\Delta G = -RT\ln(K_{Dwt}/K_{Dmut})$.

region of the β-strand/β-turn region, is good. The model, shown in Figure 7, includes the PGIP-1 LRR domain from residue 84 to 302, at which point the similarity to the plant-specific LRR consensus sequence breaks down. The model thus spans only five of the eight amino acid residue differences between PGIP-1 and PGIP-2 (H89L, G181V, A207S, K253Q and Q300H). As a consequence of adopting the βαβ plant-specific LRR fold proposed by Kajava (1998), the PGIP LRR domain models have a significant curvature, though this is less pronounced than that seen in the X-ray crystal structure of pRI (Kobe and Deisenhofer, 1993). This results from the helical portion of each repeat being shorter than in pRI and offset relative to the orientation of the β-strands. The model predicts an extensive and potentially variable ligand-binding surface facilitated by a protein fold resembling that of the β-helical structure (Kobe and Deisenhofer, 1994). As expected, the PGIP-1 and PGIP-2 model structures are very similar. The major difference arises in the region of the G181V substitution where the steric effect of the isovaleryl side chain is to reorient the side chain of the neighbouring residue, F205 (Figure 8). Differences are noted also in local main chain conformation. Elsewhere, the substitution K253Q leads to only minor local conformation differences. Structurally, the modelling suggests that the roles of these residues in modulating affinity for PG may be ascribed to steric changes at residue 181, and electrostatic and/or hydrogen bonding at position 253.

Discussion

In this work, we have investigated at the molecular level the interaction of plant PGIPs and fungal PGs. Two members (*pgip-1* and *pgip-2*) of the *pgip* gene family of *P.vulgaris* cv. Pinto have been isolated and shown to encode proteins with only eight amino acid variations in their mature form. Expression of the two genes in *N.benthamiana* using the viral vector PVX allowed the purification and characterization of the single *pgip* gene products. The two proteins exhibit distinct specificities: PGIP-1 is not able to interact with the PG of *F.moniliforme*, while PGIP-2 is and completely inhibits this enzyme. The few amino acid variations between PGIP-1 and PGIP-2 and their distinct ability to interact with *A.niger* and *F.moniliforme* PGs make these two proteins an excellent system to study the basis of recognition specificity of a LRR protein. By combining site-directed mutagenesis and SPR analysis, the contribution of each variant amino acid to the interaction with *F.moniliforme* and *A.niger* PGs has been evaluated. Our results show that single mutations of amino acid residues of PGIP-2 into the corresponding residues present in PGIP-1 cause a loss of affinity for

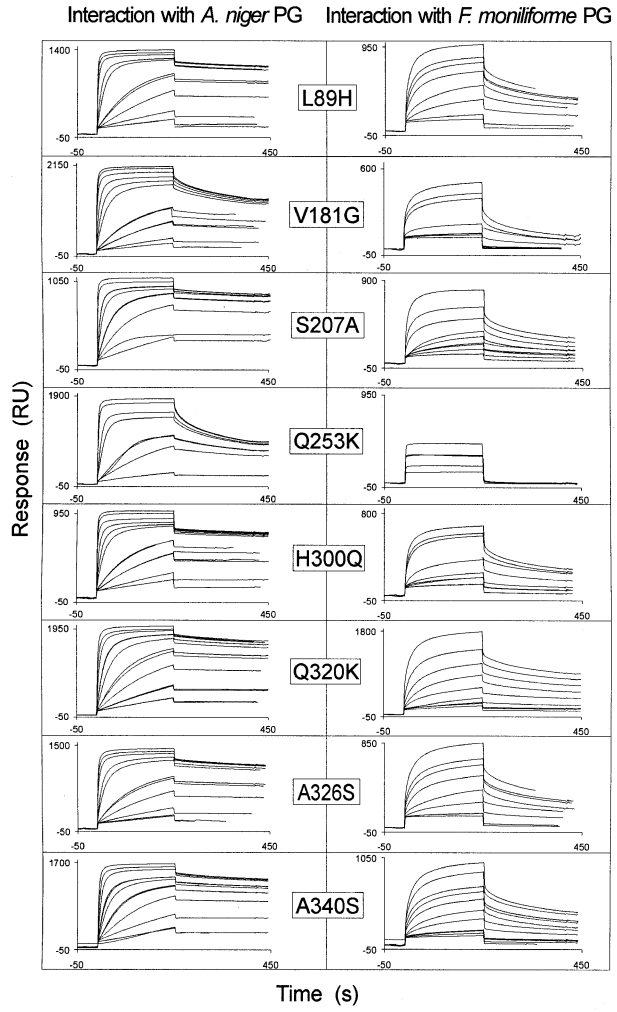

Fig. 4. Interaction between different PGIP-2 mutants and *A.niger* or *F.moniliforme* PG. The different panels show the SPR sensorgrams. (Concentrations listed from bottom to top curve.) L89H, concentrations of *A.niger* PG: 2.3, 4.6, 11, 23, 46, 114, 228 and 456 nM, and 1.1, 2.3 and 4.6 μM; concentrations of *F.moniliforme* PG: 40, 80, 160, 400 and 800 nM, and 1.6, 3.2, 4.8 and 6.4 μM. V181G, concentrations of *A.niger* PG: 2.3, 4.6, 11, 23, 46, 114, 228 and 456 nM, and 1.1, 2.3 and 3.4 μM; concentrations of *F.moniliforme* PG: 14, 40, 80, 240 and 800 nM, and 1.2 and 1.6 μM. S207A, concentrations of *A.niger* PG: 4.6, 11, 23, 46, 114 and 228 nM, and 1.1 and 2.3 μM; concentrations of *F.moniliforme* PG: 16, 40, 80, 160, 400 and 800 nM, and 1.6 and 3.2 μM. Q253K, concentrations of *A.niger* PG: 2.3, 11, 23, 114 and 228 nM, and 1.1 and 2.3 μM; concentrations of *F.moniliforme* PG: 14, 40, 80, 240 and 800 nM, and 1.2 and 1.6 μM. H300Q, concentrations of *A.niger* PG: 2.3, 4.6, 11, 23, 114, 228 and 456 nM, and 1.1, 2.3 and 3.4 μM; concentrations of *F.moniliforme* PG: 14, 40, 80, 240 and 800 nM, and 1.2 and 1.6 μM. Q320K, concentrations of *A.niger* PG: 2.3, 4.6, 11, 23, 114, 228 and 456 nM, and 1.1, 2.3 and 3.4 μM; concentrations of *F.moniliforme* PG: 14, 40, 80, 240, 400 and 800 nM, and 1.2 and 1.6 μM. A326S, concentrations of *A.niger* PG: 2.3, 4.6, 11, 23, 114, 228 and 456 nM, and 1.1, 2.3 and 3.4 μM; concentrations of *F.moniliforme* PG: 14, 40, 80, 240, 400 and 802 nM, and 1.2 and 1.6 μM. A340S, concentrations of *A.niger* PG: 2.3, 4.6, 11, 23, 114, 228 and 456 nM, and 1.1, 2.3 and 3.4 μM; concentrations of *F.moniliforme* PG: 14, 40, 80, 160, 240, 400 and 800 nM, and 1.2 and 1.6 μM. RU, resonance units.

F.moniliforme PG, with the two PGIP-2 residues Q253 and A326 accounting for nearly all the binding energy of the complex. In particular, amino acid Q253 is the major contributor to the binding energy of the complex; the replacement of Q253 with K decreases the binding energy

Table IV. Inhibition of *F.moniliforme* PG by PGIP-2 mutants

PGIP-2 mutants	% inhibition
Wild-type	100
L89H	100
V181	100
S207A	100
Q253K	30
H300Q	100
Q320K	100
A326S	100
A340S	100
V181G/Q253K	0
Q253K/A326S	0
V181G/A326S	100

The inhibition assays were carried out with 60 ng of wild-type and mutant PGIP and 0.008 U of *F.moniliforme* PG.

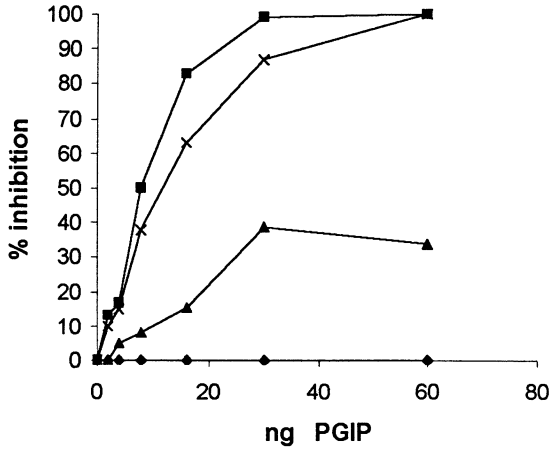

Fig. 5. Inhibition curves of homogeneous *F.moniliforme* PG by increasing amounts of PGIP-1 (◆), PGIP-2 Q253K (▲), PGIP-1 K253Q (×) and PGIP-2 (■); 0.008 U of *F.moniliforme* PG were used.

by 2.55 kcal/mol. Because, according to our structure prediction, this variation is unlikely to determine major conformational differences, Q253 may participate in the interaction by forming hydrogen bonds with residues of PG. The importance of residue Q253 is confirmed by the observation that mutation of the PGIP-1 amino acid K253 into a Q is sufficient to confer to the protein a new recognition specificity, i.e. the ability to interact with *F.moniliforme* PG. Some of the mutations of PGIP-2 also cause a decrease in affinity for *A.niger* PG, with a major contribution of the amino acids V181 and Q253.

Mutations G181V and K253Q, which determine an important change in the interaction ability of PGIP, have, according to Dayhoff *et al*. (1972), a low and moderate acceptance, respectively. This indicates that in LRR proteins, low or moderately acceptable mutability is particularly significant for the evolution of new recognition specificities. On the other hand, our data show that mutations with a high level of acceptance, such as S326A, also play a role in PGIP–PG interactions.

The residues of PG involved in the interaction with PGIP are still unknown. Recently, the three-dimensional structure of *A.niger* PG has been elucidated (Y.van Santen, J.Visser and B.W.Dijkstra, personal communication). The enzyme exhibits a β-helix structure, and, like other characterized pectic enzymes, a highly positive electro-

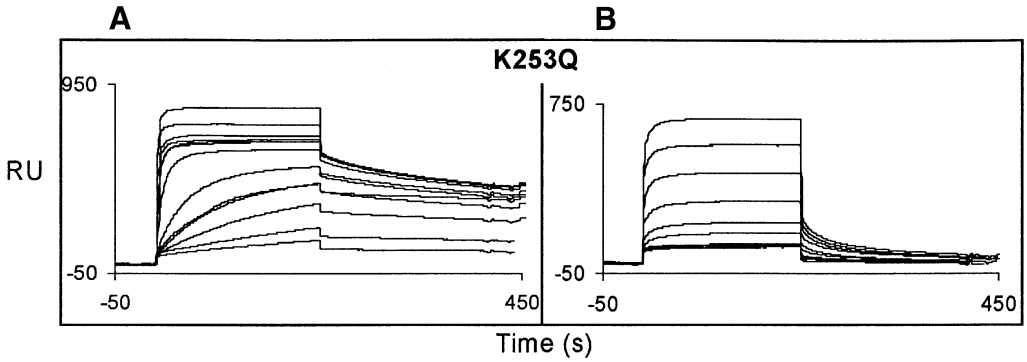

Fig. 6. Interaction between mutant PGIP-1 K253Q and *A.niger* PG (**A**) or *F.moniliforme* PG (**B**). The two panels show the SPR sensorgrams. Concentrations of *A.niger* PG (from bottom to top curve): 2.3, 4.6, 11.4, 22.8, 45.6, 114, 228 and 456 nM, and 1.1, 2.3 and 4.6 μM. Concentrations of *F.moniliforme* PG (from bottom to top curve): 40, 80, 160, 401 and 802 nM, and 1.6, 3.2, 4.8 and 6.4 μM. RU, resonance units.

static potential of the substrate-binding cleft for the binding of the polyanionic substrate polygalacturonic acid. The lysine at position 253 of PGIP-1 could contribute substantially to the specificity of binding through unfavourable electrostatic interactions, for example by repulsion of positively charged residues in non-target PGs. PGs from *A.niger* and *F.moniliforme* are 61.3% similar and only 43.4% identical (Caprari *et al.*, 1993). The ability of PGIP-2 to bind both enzymes and the observation that some residues are important for the interaction with only one PG, but not with the other, suggest that different, though overlapping, subsets of residues may be critical for binding different ligands. Interestingly, the ability of pRI to recognize different RNases has been shown to be based on its capacity to recognize a number of features unique to each enzyme (Papageorgiou *et al.*, 1997). Multiple recognition capabilities have been also described for LRR plant resistance gene products: for example, the *Arabidopsis RPM1* gene mediates recognition of two different bacterial Avr products, avrB and avrRpm1 (Grant *et al.*, 1995).

The amino acids of PGIP that determine specificity and affinity for fungal PGs are internal to the conserved xxLxLxx motif, which is predicted to form a solvent-exposed β-sheet/β-turn structure (Kobe and Deisenhofer, 1994) (Figures 7 and 8). Comparison of the sequences of *pgip-1* and *pgip-2* shows that non-synonymous nucleotide substitutions leading to amino acid variations do not occur randomly along the LRR-coding sequence but occur preferentially within or contiguous to the motif xxLxLxx. The β-sheet/β-turn region of PGIP may therefore be considered a 'hot spot' for non-synonymous variation, responsible for ligand recognition specificity. Residues in this region that appear not to be important for discriminating between *A.niger* and *F.moniliforme* PG, e.g. residues 207 and 300, perhaps are involved in the specific recognition of other ligands.

Our results provide a clear demonstration that variations in the predicted solvent-exposed β-sheet/β-turn structure of an LRR protein have a functional significance and determine the discriminatory ability for recognition of a specific ligand. Variation in the β-sheet/β-turn motif has been hypothesized to be crucial for specific recognition functions of other LRR proteins, and in particular for the products of *R* genes. For example, a glutamate to lysine substitution in the xxLxLxx of the third LRR in the

Table V. Kinetics and equilibrium of the interaction between the PGIP-1 mutant K253Q and *A.niger* or *F.moniliforme* PG

	k_{on} (per Ms)	k_{off} (per s)	K_D (nM)	ΔG (kcal/mol)
A.niger PG	2.43×10^{5}	1.5×10^{-3}	6.17	–11.19
F.moniliforme PG	3.69×10^{4}	7.59×10^{-3}	205.7	–9.12

Kinetic parameters were determined by SPR analysis. K_D values were calculated as k_{off}/k_{on}. The free energy of the formation of the complex was calculated from the equation $\Delta G = RT\ln K_D$.

Arabidopsis RPS5 gene product generates a protein which partially compromises the function of several *R* genes (Warren *et al.*, 1998). Within the tomato *Cf* gene family, the comparative analysis of Cf-4 and Cf-9, which confer resistance to *C.fulvum* through recognition of different avirulence determinants, has shown that 33 out of the 57 amino acids which distinguish the two proteins are located within the interstitial amino acid residues of the β-sheet/β-turn region (Thomas *et al.*, 1997). Also, the comparative analysis of 11 Cf-9 homologues identified 13 variable and seven hypervariable amino acid positions, the majority of which are clustered within the β-sheet/β-turn structure. Significantly, higher non-synonymous than synonymous substitution rates are observed in the nucleotide sequence corresponding to these positions, implying selection for sequence diversification of this region (Parniske *et al.*, 1997). Similar conclusions were drawn from the analysis of the *Cf-2/Cf-5* gene family (Dixon *et al.*, 1998). Other examples are the alleles of the *Arabidopsis* resistance genes *RPS2* and *RPM1*, in which single amino acid changes abolish the ability to confer resistance (Bent *et al.*, 1994; Mindrinos *et al.*, 1994; Grant *et al.*, 1995), and the genes *Xa21* of rice and *M* of flax, where alterations of the LRR domains appear to be crucial for recognition specificity (Anderson *et al.*, 1997; Ronald, 1997). Recent reports on the *RG2* and *Dm* genes in lettuce (Meyers *et al.*, 1998a,b) and on the *RPP* genes in *Arabidopsis* (Botella *et al.*, 1998; McDowell *et al.*, 1998) further support the notion that there is a divergent selection in the x residues of the xxLxLxx motif during evolution of the *R* gene products.

In conclusion, we show that, in PGIPs, sequence variability within the predicted β-sheet/β-turn structure of the LRR domain affects ligand binding and determines

Table VI. Alignment of amino acid sequences from the 10 LRRs of *P.vulgaris* PGIP-1 with the plant-specific (PS) LRR sequence as defined by Kajava (1998)

LRR	Residues	5						10						15						20						25			No.
1	84–109	**L**	D	**L**	S	G	H	**N**	L	P	K	P	Y	P	I	P	S	S	L	A	N	L	P	Y	L	N	F	–	26
2	110–134	**L**	Y	**I**	G	G	I	**N**	N	L	–	V	G	P	I	P	P	A	I	A	K	L	T	Q	L	H	Y	–	25
3	135–158	**L**	Y	**I**	T	H	–	**T**	N	V	–	S	G	A	I	P	D	F	L	S	Q	I	K	T	L	V	T	–	24
4	159–182	**L**	D	**F**	S	Y	–	**N**	A	L	–	S	G	T	L	P	P	S	I	S	S	L	P	N	L	G	G	–	24
5	183–207	**I**	T	**F**	D	G	–	**N**	R	I	–	S	G	A	I	P	D	S	Y	T	S	F	S	K	L	F	T	A	25
6	208–230	**M**	T	**I**	S	R	–	**N**	R	L	–	T	G	K	I	P	P	T	F	A	N	L	N	L	A	F	–	–	23
7	231–254	**V**	D	**L**	S	R	–	**N**	M	L	–	E	G	D	A	S	V	L	F	G	S	D	K	N	T	K	K	–	24
8	255–277	**I**	H	**L**	A	K	–	**N**	S	L	–	A	F	D	L	G	K	V	G	L	S	K	N	L	G	N	–	–	23
9	278–301	**L**	D	**L**	R	N	–	**N**	R	I	–	Y	G	T	L	P	Q	G	L	T	Q	L	K	F	L	Q	S	–	24
10	302–315	**L**	N	**V**	S	F	–	**N**	N	L	–	C	G	E	I	P	Q	G	G	N	L	K	R	F	D	V	S	S	25
PS LRR	1–24	*L*	x	*L*	x	x	–	*N*	x	*L*	–	T	*G*	x	*I*	*P*	x	x	L	G	x	L	x	x	*L*	x	x	–	24

Conserved residues in the β-strand/β-turn submotif are in bold. Residues in the PS LRR occurring at 70% or greater frequency are in italics.

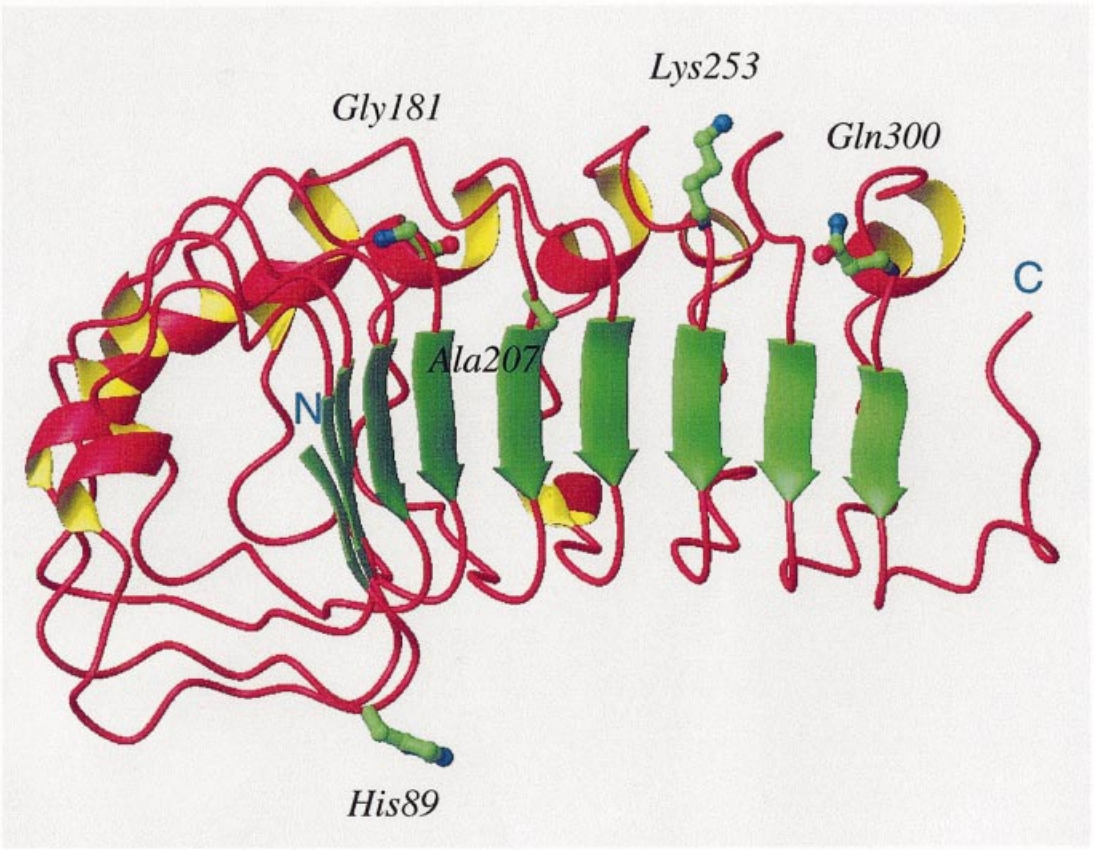

Fig. 7. The fold of modelled PGIP-1. β-Strands are shown in green and α-helices in red/yellow. The positions of the five amino acid differences between PGIP-1 and PGIP-2 that lie in the LRR domain are shown. The positions of Gly181 and Lys253 map to the heel of their respective LRR motifs preceding the β-strands.

recognition specificity. This is likely to be true in many other LRR proteins. Knowledge of the structural requirements that confer to LRR proteins the ability of interacting specifically with their ligands may allow the manipulation of the cell functions controlled by these proteins. Strategies for *in vitro* mutagenesis can be envisaged to obtain more efficient PGIPs, or PGIPs with novel recognition abilities for specific target molecules. More generally, the information gained on PGIP may open the way to a 'directed' manipulation of those LRR receptor proteins which are structurally related to PGIP and are involved in both the development and resistance of plants.

Materials and methods

Screening of the cDNA library

Construction and screening of the cDNA library of *P.vulgaris* cv. Pinto have been described previously (Toubart *et al.*, 1992).

Nucleic acid manipulations

Standard techniques were used for recombinant DNA work (Sambrook *et al.*, 1989). Dideoxy DNA sequencing was carried out using the Sequenase-2 kit (US Biochemicals, Cleveland, OH). Oligonucleotides were synthesized by M-Medical, Florence, Italy.

Preparation of vectors for gene expression using PVX

The *pgip-1* sequences including the first ATG up to 200 nucleotides downstream of the stop codon were amplified by PCR using sequence-

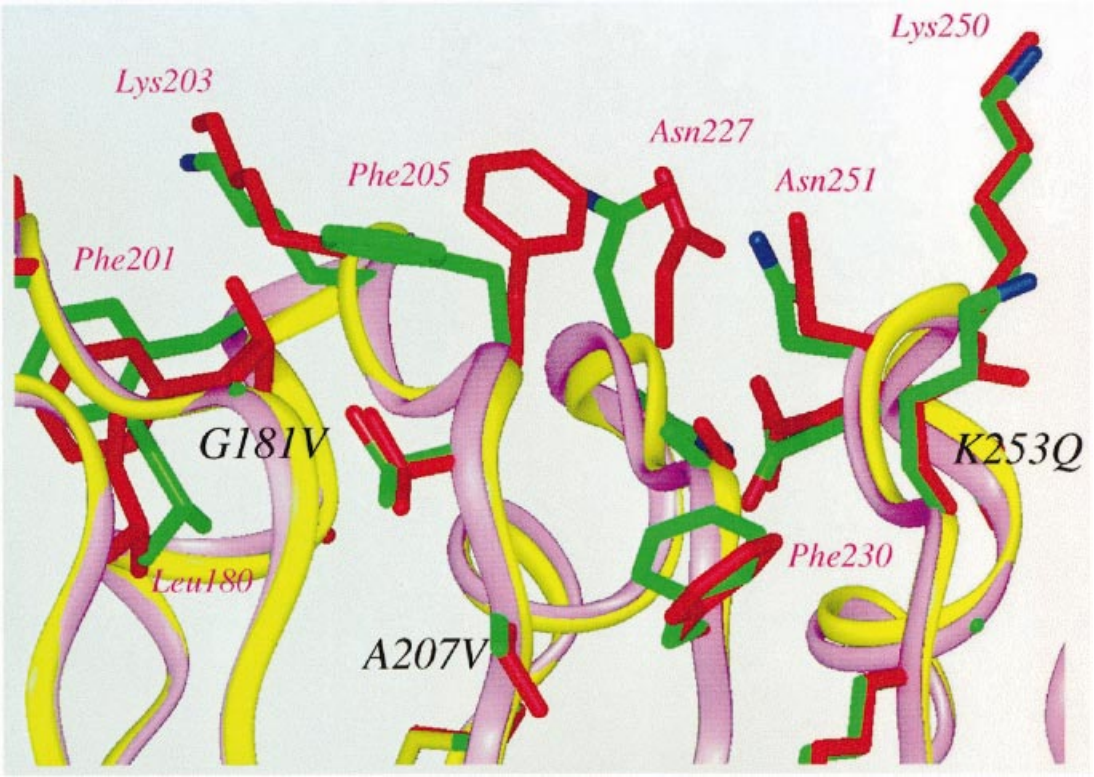

Fig. 8. A close up of a least-squares superposition of modelled PGIP-1 and PGIP-2 structures showing the region around residues 181, 207 and 253. The main chain ribbon of PGIP-1 is magenta, that of PGIP-2, yellow. Side chains that show the most significant conformational differences between the two structures are shown. The side chains of residues of PGIP-2 are red.

specific oligonucleotides with the *Cla*I and *Sal*I sites included at the 5′ end to facilitate cloning. The amplified fragment was repaired and cloned in the *Eco*RV site of pBlueScript SK+ to create pBS11. The *pgip-1* sequence contains two in-frame ATGs while the *pgip-2* cDNA clone contains only the second ATG and lacks the preceding sequences. These 5′ sequences of the *pgip* gene appear to be important for expression levels (Devoto *et al.*, 1998). In order to attach the first ATG and the intermediate sequences to *pgip-2*, a *Hin*dIII endonuclease restriction site contained in the DNA sequences corresponding to the signal peptide (Figure 1) was used to facilitate the substitution of the *pgip-1* coding sequence with that of *pgip-2*. pBS11 was digested with *Hin*dIII–*Sal*I and the vector containing the 5′ sequences of *pgip-1* recovered. The *pgip-2* cDNA clone was digested with *Hin*dIII–*Sal*I to excise the coding sequences which were ligated into the recovered vector. This created the recombinant plasmid pBS23 containing the coding sequences of *pgip-2* with two in-frame ATGs. The *pgip-2* gene fragments were excised from pBS23 using *Cla*I and *Sal*I and inserted in the pPVX201 PVX expression vector (Baulcombe *et al.*, 1995) to generate the plasmid PVX.PGIP-2. The generation of PVX.PGIP-1 was as described previously (Desiderio *et al.*, 1997).

Chimeric genes *pgip-12* and *pgip-21* were constructed using the unique *Mlu*I site present in the *pgip* gene. pBS11 and pBS23 were digested with *Mlu*I–*Pst*I and subjected to agarose electrophoresis. The excised fragment of 500 bp from pBS11 was then ligated with the large fragment of 3.3 kb deriving from the digestion of pBS23 to create *pgip-21*. Then the small fragment of 500 bp deriving from the digestion of pBS23 was ligated with the large fragment from pBS11 to create *pgip-12*. The chimeric genes were ligated, following a double digestion with *Cla*I–*Sal*I in pPVX201 as described for *pgip-2* to create PVX.PGIP12 and PVX.PGIP21.

Site-directed mutagenesis of the pgip genes

A commercial site mutagenesis kit (U.S.E) and protocols were used (Pharmacia P-L Biochemicals Inc). The mutagenesis of the *pgip-2* gene was carried out on the plasmid pBS23, using the following loss-of-function primers which mutated an amino acid in PGIP-2 to the corresponding amino acid in PGIP-1: PL89H, 5′-GACCTCTCCGG-CCATAACCTCCCAAAAC-3′; PV181G, 5′-CTCCCCAACCTCGGA-GGAATCACATTC-3′; PS207A, 5′-GAAGCTGTTTACGGCGATGAC-CATCTCC-3′; PQ253K, 5′-CAGATAAGAACACGAAGAAGATAC-ATCTGGC-3′; PH300Q, 5′-GCAGCTAAAGTTTCTGCAAAGTTTAA-ATGTGAGCTTC-3′; PQ320K, 5′-GGTGGGAACTTGAAAAGGTT-TGACGTTTC-3′; PA326S, 5′-GTTTGACGTTTCTTCTTATGCCAA-CAACAAG-3′; PA340S, 5′-GTTCTCCTCTTCCTTCCTGCACTTA-ACA-3′.

The mutagenesis of the *pgip-1* gene was carried out on the plasmid pBS11, using the following gain-of-function primer which mutated the amino acid in PGIP-1 to the corresponding amino acid in PGIP-2: PK253Q, 5′-CAGATAAGAACACGCAGAAGATACATCTGGC-3′.

The selection primer which mutated the *Sst*I restriction enzyme site was as follows: pBSSST1, 5′-GTGGTACCGAGCCCGGTACCCCATG-3′.

Following mutagenesis, the genes were *Cla*I–*Sal*I ligated into pPVX201 for heterologous expression in *N.benthamiana*. The plasmid pPVX201 contains the cauliflower mosaic virus (CaMV) 35S promoter and plasmid DNA was used to inoculate *N.benthamiana* plants directly using 30 μg of DNA/plant as described previously (Baulcombe *et al.*, 1995).

Preparation and assay of PGs and PGIPs

PGII from *A.niger* was prepared as described by Kester and Visser (1990), PG of *F.moniliforme* expressed in *S.cerevisiae* was prepared as described by Caprari *et al.* (1996) and PGs from *B.cinerea* and *F.oxysporum* f.sp. *lycopersici* were prepared as described by Desiderio *et al.* (1997). PGIP-1, PGIP-2 and the mutant PGIPs were purified from PVX-infected tissues of *N.benthamiana* by an affinity-based procedure on a Sepharose–*A.niger* PG column as described previously (Cervone *et al.*, 1987). PG and PGIP activities were measured with the standard PAHBAH assay as already described (Cervone *et al.*, 1989).

SPR

SPR measurements were conducted as already described (Desiderio *et al.*, 1997).

Modelling of PGIPs

Construction of the model of *P.vulgaris* PGIP-1 was carried out using the program InsightII (Biosym Technologies Inc., San Diego, CA) running on a Silicon Graphics Indigo^2 XZ workstation. The template for the single 24 amino acid LRR came from the plant-specific LRR

motif model of Kajava (1998). A framework for the structure of PGIP-1 was constructed by replicating this motif structure to give a tandem array of 10 identical LRRs. The sequences of the LLR motifs from PGIP-1 were then aligned manually with the plant-specific LRR sequence. For the LRRs of 24 amino acids, the modelling process was straightforward and involved substitution of the corresponding amino acid type. For the remaining LRRs, the conformations of loops connecting secondary structural elements were modelled by searching a database of loop conformations generated from high-resolution protein structures. Amino acid side chain conformations were selected by knowledge of their torsional preferences. Construction of the starting model for PGIP-2 followed, by simple substitution of the amino acids at positions differing between the two proteins within the LRR domain (H89L, G181V, A207S, K253Q and Q300H). Both models were then subjected to energy minimization using the program X-PLOR (Brunger *et al.*, 1987). Two rounds of steepest descent optimization (250 cycles each) were performed, with harmonic restraints (force constant $K_{restraint}$ = 20 kcal/mol/Å^2) applied to all main chain atoms. The restraint coordinates were updated after each round. The final step involved 1500 cycles of unrestrained conjugate gradient optimization. A unitary dielectric constant was used throughout.

Acknowledgements

The authors would like to thank Dr David Baulcombe (Sainsbury Laboratory, John Innes Institute, Norwich, UK) for the kind gift of the PVX expression system, and Dr J.Benen (Section of Molecular Genetics, Department of Genetics, Agricultural University, Wageningen, The Netherlands) for the generous gift of PGII from *A.niger*. This research was supported by the European Community Grants BIO4-CT96-515 and BIO4-CT96-685, the Institute Pasteur-Fondazione Cenci Bolognetti and the Giovanni Armenise-Harvard Foundation.

References

Anderson,P.A., Lawrence,G.J., Morrish,B.C., Alyffe,M.A., Finnegan,J. and Ellis,J.G. (1997) Inactivation of the flax rust resistance gene *M* associated with loss of a repeated unit within the leucine-rich repeat coding region. *Plant Cell*, **9**, 641–651.

Baulcombe,D., Chapman,S. and Santa Cruz,S. (1995) Jellyfish green fluorescent protein as a reporter for virus infections. *Plant J.*, **7**, 1045–1053.

Bent,A.F. (1996) Plant disease resistance genes: function meets structure. *Plant Cell*, **8**, 1757–1771.

Bent,A.F., Kunkel,B.N., Dahlbeck,D., Brown,K.L., Schmidt,R., Giraudat,J., Leung,J. and Staskawicz,B.J. (1994) *RPS2* of *Arabidopsis thaliana*: a leucine-rich repeat class of plant disease resistance genes. *Science*, **265**, 1856–1860.

Botella,M.A., Parker,J.E., Frost,L.N., Bittner-Eddy,P.D., Beynon,J.L., Daniels,M.J., Holub,E.B. and Jones,J.D.G. (1998) Three genes of the *Arabidopsis RPP1* complex resistance locus recognize distinct *Peronospora parasitica* avirulence determinants. *Plant Cell*, **10**, 1847–1860.

Brunger,A.T., Kuriyan,J. and Karplus,M. (1987) X-PLOR version 3.1: a system for X-ray and NMR. *Science*, **235**, 458.

Buchanan,S.G.S. and Gay,N.J. (1996) Structural and functional diversity in the leucine-rich repeat family of proteins. *Prog. Biophys. Mol. Biol.*, **65**, 1–44.

Caprari,C., Richter,A., Bergmann,C., Lo Cicero,S., Salvi,G., Cervone,F. and De Lorenzo,G. (1993) Cloning and characterization of the gene encoding the endopolygalacturonase of *Fusarium moniliforme*. *Mycol. Res.*, **97**, 497–505.

Caprari,C., Mattei,B., Basile,M.L., Salvi,G., Crescenzi,V., De Lorenzo,G. and Cervone,F. (1996) Mutagenesis of endopolygalacturonase from *Fusarium moniliforme*: histidine residue 234 is critical for enzymatic and macerating activities and not for binding to polygalacturonase-inhibiting protein (PGIP). *Mol. Plant Microbe Interact.*, **9**, 617–624.

Cervone,F., De Lorenzo,G., Degra,L., Salvi,G. and Bergami,M. (1987) Purification and characterization of a polygalacturonase-inhibiting protein from *Phaseolus vulgaris* L. *Plant Physiol.*, **85**, 631–637.

Cervone,F., Hahn,M.G., De Lorenzo,G., Darvill,A. and Albersheim,P. (1989) Host–pathogen interactions. XXXIII. A plant protein converts a fungal pathogenesis factor into an elicitor of plant defense responses. *Plant Physiol.*, **90**, 542–548.

Cervone,F., Castoria,R., Leckie,F. and De Lorenzo,G. (1997) Perception of fungal elicitors and signal transduction. In Aducci,P. (ed.), *Signal Transduction in Plants*. Birkauser Verlag, Basel, Switzerland, pp. 153–177.

Clark,S.E., Williams,R.W. and Meyerowitz,E.M. (1997) The *CLAVATA1* gene encodes a putative receptor kinase that controls shoot and floral meristem size in *Arabidopsis*. *Cell*, **89**, 575–585.

Dayhoff,M.O., Eck,R.V. and Park,C.M. (1972) A model of evolutionary change in proteins. In Dayhoff,M.O. (ed.), *Atlas of Protein Sequence and Structure*. Vol. 5. National Biomedical Research Foundation, Georgetown University Medical Center, Washington, DC, pp. 89–99.

De Lorenzo,G. and Cervone,F. (1997) Polygalacturonase-inhibiting proteins (PGIPs): their role in specificity and defense against pathogenic fungi. In Stacey,G. and Keen,N.T. (eds), *Plant–Microbe Interactions*. Vol. 3. Chapman & Hall, New York, NY, pp. 76–93.

Desiderio,A. *et al*. (1997) Polygalacturonase-inhibiting proteins (PGIPs) with different specificities are expressed in *Phaseolus vulgaris*. *Mol. Plant Microbe Interact.*, **10**, 852–860.

Devoto,A., Leckie,F., Lupotto,E., Cervone,F. and De Lorenzo,G. (1998) The promoter of a gene encoding PGIP (PolyGalacturonase-Inhibiting Protein) of *Phaseolus vulgaris* L. is activated by wounding but not by elicitors or pathogen infection. *Planta*, **205**, 165–174.

Dixon,M.S., Hatzixanthis,K., Jones,D.A., Harrison,K. and Jones,J.D.G. (1998) The tomato *Cf-5* disease resistance gene and six homologs show pronounced allelic variation in leucine-rich repeat copy number. *Plant Cell*, **10**, 1915–1925.

Favaron,F., D'Ovidio,R., Porceddu,E. and Alghisi,P. (1994) Purification and molecular characterization of a soybean polygalacturonase-inhibiting protein. *Planta*, **195**, 80–87.

Frediani,M., Cremonini,R., Salvi,G., Caprari,C., Desiderio,A., D'Ovidio,R., Cervone,F. and De Lorenzo,G. (1993) Cytological localization of the *pgip* genes in the embryo suspensor cells of *Phaseolus vulgaris* L. *Theor. Appl. Genet.*, **87**, 369–373.

Grant,M.R., Godiard,L., Straube,E., Ashfield,T., Lewald,J., Sattler,A., Innes,R.W. and Dangl,J.L. (1995) Structure of the *Arabidopsis RPM1* gene enabling dual specificity disease resistance. *Science*, **269**, 843–846.

Granzow,R. and Reed,R. (1992) Interactions in the fourth dimension. *Biotechnology*, **10**, 390–393.

Hammond-Kosack,K.E. and Jones,J.D.G. (1997) Plant disease resistance genes. *Annu. Rev. Plant Physiol. Plant Mol. Biol.*, **48**, 575–607.

Johnston,D.J., Ramanathan,V. and Williamson,B. (1993) A protein from immature raspberry fruits which inhibits endopolygalacturonases from *Botrytis cinerea* and other micro-organisms. *J. Exp. Bot.*, **44**, 971–976.

Kajava,A.V. (1998) Structural diversity of leucine-rich repeat proteins. *J. Mol. Biol.*, **277**, 519–527.

Kester,H.C.M. and Visser,J. (1990) Purification and characterization of polygalacturonases produced by the hyphal fungus *Aspergillus niger*. *Biotechnol. Appl. Biochem.*, **12**, 150–160.

Kobe,B. and Deisenhofer,J. (1993) Crystal structure of porcine ribonuclease inhibitor, a protein with leucine-rich repeats. *Nature*, **366**, 751–756.

Kobe,B. and Deisenhofer,J. (1994) The leucine-rich repeat: a versatile binding motif. *Trends Biochem. Sci.*, **19**, 415–421.

Kobe,B. and Deisenhofer,J. (1995) A structural basis of the interactions between leucine-rich repeats and protein ligands. *Nature*, **374**, 183–186.

Kobe,B. and Deisenhofer,J. (1996) Mechanism of ribonuclease inhibition by ribonuclease inhibitor protein based on the crystal structure of its complex with ribonuclease A. *J. Mol. Biol.*, **264**, 1028–1043.

Kresse,H., Liszio,C., Schonherr,E. and Fisher,L.W. (1997) Critical role of glutamate in a central leucine-rich repeat of decorin for interaction with type I collagen. *J. Biol. Chem.*, **272**, 18404–18410.

Li,J.M. and Chory,J. (1997) A putative leucine-rich repeat receptor kinase involved in brassinosteroid signal transduction. *Cell*, **90**, 929–938.

McDowell,J.M., Dhandaydham,M., Long,T.A., Aarts,M.G.M., Goff,S., Holub,E.B. and Dangl,J.L. (1998) Intragenic recombination and diversifying selection contribute to the evolution of downy mildew resistance at the *RPP8* locus of *Arabidopsis*. *Plant Cell*, **10**, 1861–1874.

Meyers,B.C., Chin,D.B., Shen,K.A., Sivaramakrishnan,S., Lavelle,D.O., Zhang,Z. and Michelmore,R.W. (1998a) The major resistance gene cluster in lettuce is highly duplicated and spans several megabases. *Plant Cell*, **10**, 1817–1832.

Meyers,B.C., Shen,K.A., Rohani,P., Gaut,B.S. and Michelmore,R.W. (1998b) Receptor-like genes in the major resistance locus of lettuce are subject to divergent selection. *Plant Cell*, **10**, 1833–1846.

Mindrinos,M., Katagiri,F., Yu,G.-L. and Ausubel,F.M. (1994) The *A.thaliana* disease resistance gene *RPS2* encodes a protein containing a nucleotide-binding site and leucine-rich repeats. *Cell*, **78**, 1089–1099.

Papageorgiou,A.C., Shapiro,R. and Acharya,K.R. (1997) Molecular recognition of human angiogenin by placental ribonuclease inhibitor—an X-ray crystallographic study at 2.0 Å resolution. *EMBO J.*, **16**, 5162–5177.

Parniske,M., Hammond-Kosack,K.E., Golstein,C., Thomas,C.M., Jones, D.A., Harrison,K., Wulff,B.B.H. and Jones,J.D.G. (1997) Novel disease resistance specificities result from sequence exchange between tandemly repeated genes at the *Cf-4/9* locus of tomato. *Cell*, **91**, 821–832.

Puett,D., Bhowmick,N., Fernandez,L.M., Huang,J., Wu,C. and Narayan,P. (1996) hCG-receptor binding and transmembrane signaling. *Mol. Cell. Endocrinol.*, **125**, 55–64.

Ronald,P.C. (1997) The molecular basis of disease resistance in rice. *Plant Mol. Biol.*, **35**, 179–186.

Sambrook,J., Fritsch,E.F. and Maniatis,T. (1989) *Molecular Cloning: A Laboratory Manual*. Cold Spring Harbor Laboratory Press, Cold Spring Harbor, NY.

Schuster,S.C., Swanson,R.V., Alex,L.A., Bourret,R.B. and Simon,M.I. (1993) Assembly and function of a quaternary signal transduction complex monitored by surface plasmon resonance. *Nature*, **365**, 343–347.

Stotz,H.U., Powell,A.L.T., Damon,S.E., Greve,L.C., Bennett,A.B. and Labavitch,J.M. (1993) Molecular characterization of a polygalacturonase inhibitor from *Pyrus communis* L. cv Bartlett. *Plant Physiol.*, **102**, 133–138.

Stotz,H.U., Contos,J.J.A., Powell,A.L.T., Bennett,A.B. and Labavitch, J.M. (1994) Structure and expression of an inhibitor of fungal polygalacturonases from tomato. *Plant Mol. Biol.*, **25**, 607–617.

Thomas,C.M., Jones,D.A., Parniske,M., Harrison,K., Balint-Kurti,P.J., Hatzixanthis,K. and Jones,J.D.G. (1997) Characterization of the tomato *Cf-4* gene for resistance to *Cladosporium fulvum* identifies sequences that determine recognitional specificity in Cf-4 and Cf-9. *Plant Cell*, **9**, 2209–2224.

Thomas,D., Rozell,T.G., Liu,X.B. and Segaloff,D.L. (1996) Mutational analyses of the extracellular domain of the full-length lutropin/choriogonadotropin receptor suggest leucine-rich repeats 1–6 are involved in hormone binding. *Mol. Endocrinol.*, **10**, 760–768.

Torii,K.U., Mitsukawa,N., Oosumi,T., Matsuura,Y., Yokoyama,R., Whittier,R.F. and Komeda,Y. (1996) The *Arabidopsis ERECTA* gene encodes a putative receptor protein kinase with extracellular leucine-rich repeats. *Plant Cell*, **8**, 735–746.

Toubart,P., Desiderio,A., Salvi,G., Cervone,F., Daroda,L., De Lorenzo,G., Bergmann,C., Darvill,A.G. and Albersheim,P. (1992) Cloning and characterization of the gene encoding the endopolygalacturonase-inhibiting protein (PGIP) of *Phaseolus vulgaris* L. *Plant J.*, **2**, 367–373.

Wang,G.L., Song,W.Y., Ruan,D.L., Sideris,S. and Ronald,P.C. (1996) The cloned gene, *Xa21*, confers resistance to multiple *Xanthomonas oryzae* pv *oryzae* isolates in transgenic plants. *Mol. Plant Microbe Interact.*, **9**, 850–855.

Warren,R.F., Henk,A., Mowery,P., Holub,E. and Innes,R.W. (1998) A mutation within the leucine-rich repeat domain of the *Arabidopsis* disease resistance gene *RPS5* partially suppresses multiple bacterial and downy mildew resistance genes. *Plant Cell*, **10**, 1439–1452.

Received January 11, 1999; revised and accepted March 4, 1999